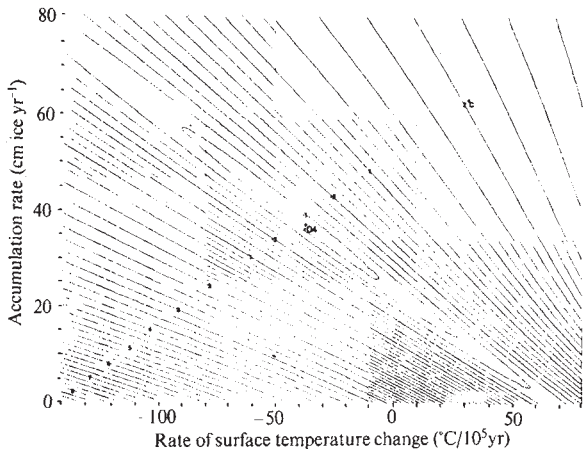

Fig. 2 Standard deviation of difference between observed and computed temperatures (°C) for Camp Century, Greenland.

gradient along the ice surface, and changes in the elevation of the cap surface as well as in climatic conditions.

Solutions for a variety of forms of the heat conduction equation have been found for all combinations of these parameters in the ranges shown in Fig. 2, which is a computer output of one of the error standard deviation fields obtained. The best combinations of accumulation and rate of surface temperature change lie in a narrow diagonal band such that an increase of 1 cm yr^{-1} in the accumulation rate has a similar effect to a decrease of 3° C/10^5 yr in the surface warming rate. The optimum fit for the Camp Century temperatures has a standard deviation of 0.04° C; the corresponding errors are shown enlarged on the right in Fig. 1 and (apart from the disturbed top layer) lack any systematic trend. The optimum fit occurs for a surface accumulation of 36 cm ice yr^{-1} almost exactly the currently observed rate. A similar conclusion has been reached from corresponding analyses of the Byrd temperatures.

But it is the implied rate of surface temperature change which represents the most significant of this type of analysis. Its value for the slowly moving ice of the Camp Century region, −37° C/10^5 yr, suggests a long-term climatic cooling at the rate of about 5° in 10,000 yr, a surface rise at the rate of 4–5 cm yr^{-1}, or some combination of these two effects. A fuller discussion covering the different models and assumptions used in the temperature calculations will be given elsewhere. This preliminary account is to establish that the observed temperatures can be reconciled with currently observed accumulation rates, and to demonstrate the diagnostic content of both the existing information on ice temperature and that promised by future deep drillings in Greenland and Antarctica.

We thank Mr T. H. Jacka for carrying out the calculations.

W. F. Budd

Antarctic Division,
Department of Supply,

D. Jenssen
U. Radok

Meteorology Department,
University of Melbourne

Received June 8, 1971.

[1] Hansen, B. L., and Langway, jun., C. C., *Antarctic J. US*, **1**, 207 (1966).
[2] Weertman, J., *J. Geophys. Res.*, **73**, 2691 (1968).
[3] Dansgaard, W., and Johnsen, S. J., *J. Geophys. Res.*, **74**, 1109 (1969).
[4] Langway, jun., C. C., *US Army Cold Regions Research and Engineering Laboratory Res. Rep. No. 77* (1967).
[5] Philberth, K., and Federer, B., *J. Glaciol.*, **10**, 3 (1971).
[6] Robin, G. de Q., *Intern. Assoc. Scientific Hydrology Publ. No. 86*, 141 (1970).
[7] Robin, G. de Q., *J. Glaciol.*, **2**, 523 (1955).
[8] Budd, W. F., *Australian National Antarctic Research Expedition Scientific Rep. A(IV) Publ. 108* (1969).
[9] Radok, U., Jenssen, D., and Budd, W. F., *Intern. Assoc. Scientific Hydrology Publ. No. 86*, 151 (1970).
[10] Ueda, H. T., and Garfield, D. E., *Intern. Assoc. Scientific Hydrology Publ. No. 86*, 53 (1970).

Flow Law for Antarctic Ice Shelves

Ice shelves are floating glaciers which are attached to an inland ice sheet or to land. They creep under their own weight, the creep rates being dependent on the ice flow law at low stresses.

Early laboratory studies[1,2] of the steady state creep of polycrystalline ice in uniaxial compression gave a power law relating strain rate ($\dot{\varepsilon}$) and applied stress (σ):

$$\dot{\varepsilon} = K\sigma^n \qquad (1)$$

where K is a temperature-dependent constant of the form $Ae^{-Q/RT}$, and n appeared to be stress-dependent, ranging from 1 at stresses well below 0.1 MN m^{-2} to 3 or 4 for stresses between 0.1 and 2 MN m^{-2}.

Particularly at low stresses, however, it is difficult to distinguish steady state creep from transient creep. True steady state creep rates can best be deduced by applying transient creep theory to the observed creep-time curve. Using this method, Walker[3] and Tabor and Walker[4] concluded that a power law with $n=3$ fits the available data over the stress range $\sigma=0.1$ to 2 MN m^{-2}, and that there is no reliable laboratory evidence for Newtonian flow ($n=1$) at low stresses. Indeed laboratory experiments at stresses below 0.1 MN m^{-2} become excessively time consuming, and it is in this region that field glaciology is likely to supply more information.

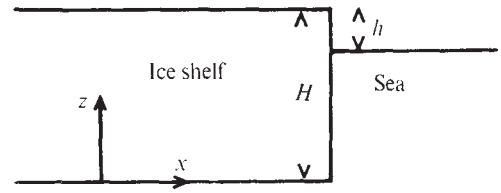

Fig. 1 Cross section of an ice shelf.

Neglecting elastic strains, Odqvist's generalization (see, for example, ref. 5) to three dimensions of the uniaxial flow law can be written:

$$\dot{\gamma} = (\tau/B)^n \qquad (2)$$

where $2\dot{\gamma}^2$ and $2\tau^2$ are the second invariants of the strain rate and stress deviator tensors respectively; $\dot{\gamma}$ is the effective shear strain rate and τ is the effective shear stress. B can be expressed in terms of K and n. The strain rate in any direction x then becomes:

$$\dot{\varepsilon}_{xx} = \left(\frac{\tau}{B}\right)^{n-1} \cdot \frac{\sigma'_{xx}}{B} \qquad (3)$$

where σ_{xx} is the stress deviator in the x direction.

Using this relationship many attempts[6–8] have been made to deduce the parameters B and n from the observed behaviour of glaciers, but difficulty arises either from the use of an oversimplified theoretical model or from lack of knowledge of all the relevant field data. Many of the published results show an apparent trend towards Newtonian flow at low stresses, but the errors are so large that no firm conclusion can be reached.

We can reduce these errors if we consider the behaviour of floating ice shelves, which represent perhaps the simplest

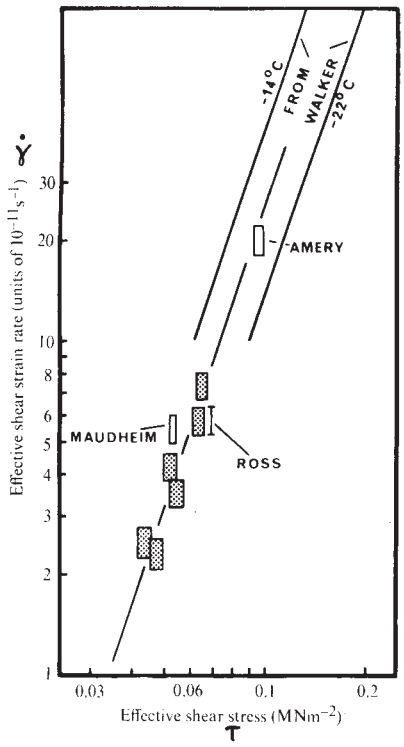

Fig. 2 Log–log plot of shear stress against shear strain rate for ice shelves of differing thickness. The unlabelled points are from the Brunt Ice Shelf.

natural ice forms. They rest on a frictionless bed, stress conditions are uniform over large distances, and boundary conditions at the upper and lower surfaces are known. For an ice shelf of constant thickness (H) we have zero shear stresses of the type σ_{ij} if we choose x and y axes horizontal and z axis vertical (Fig. 1). τ then reduces to $(\sigma_{xx}-\sigma_{zz})$ times a constant which depends on the ratio between the horizontal components of strain rate, and is equal to $\frac{1}{2}$ for the case of zero strain in the y direction. By balancing σ_{xx} integrated over depth against seawater pressure at the ice front, Weertman[9] has shown that, for an ice shelf of uniform density ρ,

$$(\sigma_{xx} - \sigma_{zz}) = \frac{\rho g h}{2} \qquad (4)$$

where h is the elevation above sea level of the ice shelf top surface. In the more usual case of ρ increasing with depth:

$$(\sigma_{xx} - \sigma_{zz}) = \frac{g}{H}\left\{\int_0^H \int_z^H \rho(z)\,dz\,dz - \tfrac{1}{2}\rho_w(H-h)^2\right\} \qquad (5)$$

where ρ_w is the density of sea water.

Applying Weertman's solution to data from several ice shelves of differing thickness[10–13], but approximately the same mean temperature, we plot log $\dot{\gamma}$ against log τ to obtain a straight line of slope n (Fig. 2). The line represented by $n=3$ fits the data well, implying a behaviour consistent with Walker's laboratory results at stresses down to 0.04 MN m^{-2}.

The lower stress region of Walker's results for $-14°$ C and $-22°$ C is included in Fig. 2 for comparison. Most of the scatter of the ice shelf results can be attributed to differences between the mean temperatures (and hence the values of B) of the various ice shelves. With $n=3$ in equation (2) we calculate values of B averaged over depth ($\bar{B}$) for each of the four ice shelves; the results are plotted against mean ice shelf temperature (obtained from measurements of temperature at depth) in Fig. 3. Also shown is a B–T graph deduced from Walker's laboratory results, and theoretical values of $\bar{B}$ calculated for each ice shelf using this graph and the known, or assumed, variation of temperature with depth. (In calculating the mean ice shelf temperatures and theoretical values of $\bar{B}$, temperatures in the upper 40 m of low density, relatively soft firn have been neglected). Although the agreement is good, it is significant that, apart from at Maudheim, the field values of $\bar{B}$ are larger than expected and the ice shelves appear harder than laboratory ice at the same temperature. This is believed to be because conditions at Maudheim most closely approach those of a freely floating ice shelf, while in the other three cases the ice is shearing past either grounded ice or ice shelf moving at a different velocity, and part of the driving force assumed to be responsible for creep is being lost in transverse shear. Weertman's equations for an unconfined ice shelf can be generalized to the case of an ice shelf restrained between parallel sides, and the resultant expression has been applied to the Amery Ice Shelf data to give improved values of $\bar{B}$ which are also shown in Fig. 3.

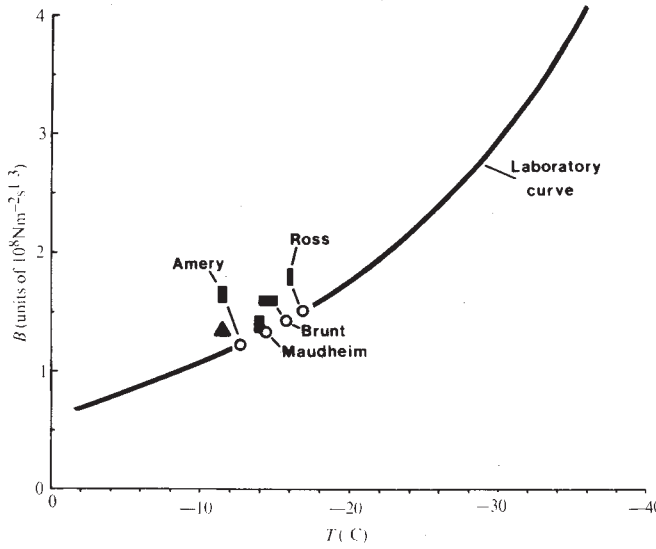

Fig. 3 Plot of the ice flow law parameter B against temperature. Ice shelf values of B meaned over depth (■) assuming unconfined 'Weertman' creep are compared with those (○) deduced from Walker's laboratory B–T curve. The restraining effects of the ice shelf sides imply a reduced value of $\bar{B}$ (▲) for the Amery Ice Shelf.

Walker's laboratory results apply to polycrystalline ice with no preferred orientation. After prolonged stress, dynamic recrystallization occurred, new grains forming with the c-axes aligned perpendicular to the resolved shear stress (45° to the stress axes in the case of uniaxial compression). This is accompanied by pronounced softening of the ice sample, and the steady state flow law no longer applies. In the absence of dynamic recrystallization we should expect the c-axes to be slowly tilted to become parallel to the compressive stress axis[14,15], thus hardening the specimen. This is seldom observed in the laboratory experiments, which by necessity are of relatively short duration, but under conditions of low stress and large total strain such as occur in glaciers the effects of grain tilting may become appreciable.

At Maudheim no trend towards a preferred orientation was found down to a depth of 100 m[16]. But at Little America on the Ross Ice Shelf, Gow[17] reported a gradual migration of c-axes towards the vertical, and at 116 m depth 75% of the c-axes were oriented within 35° of the vertical. At greater depths the c-axes clustered in three or four maxima symmetrically situated generally within 25° of the vertical. This could represent a state of equilibrium between the simultaneous effects of both dynamic recrystallization and grain tilting. Dynamic recrystallization would tend to predominate in the warmer ice near the base of the ice shelf, but we know that at Little America this ice is continually melting away[11]. Although the preferred

fabric of the Ross Ice Shelf core may to some extent explain the slightly high values of $\bar{B}$ deduced from strain rates measured at Little America, its effect is relatively small.

The agreement between laboratory results and those from ice shelves suggests that a generalized flow low, $\dot{\gamma} = \left(\frac{\tau}{B}\right)^n$, relating shear strain rate to shear stress can be applied with $n \simeq 3$ at least over the stress range 1 MN m^{-2} > τ > 0.04 MN m^{-2}. To extend this range below 0.04 MN m^{-2} would require data from ice shelves thinner than those considered here.

I thank the British Antarctic Survey for sponsoring this work, Professor J. Weertman for helpful suggestions and members of Scott Polar Research Institute for reading and improving the manuscript.

R. H. THOMAS

British Antarctic Survey,
Scott Polar Research Institute,
Lensfield Road,
Cambridge

Received June 21, 1971.

1 Glen, J. W., *Proc. Roy. Soc.*, A, **228**, 519 (1955).
2 Steinemann, S., *Int. Assoc. Sci. Hydrol.*, **39**, 449 (1954).
3 Walker, J. C. F., thesis, University of Cambridge (1970).
4 Tabor, D., and Walker, J. C. F., *Nature*, **228**, 137 (1970).
5 Odqvist, F. K. G., *Mathematical Theory of Creep and Creep Rupture* (Clarendon Press, Oxford, 1966).
6 Nye, J. F., *Proc. Roy. Soc.*, A, **219**, 477 (1953).
7 Paterson, W. S. B., and Savage, J. C., *J. Geophys. Res.*, **68**, 4537 (1963).
8 Holdsworth, G., and Bull, C., *Int. Assoc. Sci. Hydrol.*, **86**, 204 (1970).
9 Weertman, J., *J. Glaciol.*, **3**, 38 (1957).
10 Swithinbank, C. W. M., *Norw.-Brit.-Swed. Ant. Exp., Sci. Res.*, **3**, 77 (Norsk Polarinstitutt, Oslo, 1958).
11 Crary, A. P., *IGY Glaciol. Rep. Series*, **5** (1961).
12 Budd, W., *J. Glaciol.*, **6**, 335 (1966).
13 Thomas, R. H., *Survey Review*, **20**, 322 (1970).
14 Schmid, E., and Boas, W., *Plasticity of Crystals* (Chapman and Hall, London, 1968).
15 Glen, J. W., *J. Glaciol.*, **2**, 111 (1952).
16 Schytt, V., *Norw.-Brit.-Swed. Ant. Exp., Sci. Res.*, **4**, 115 (Norsk Polarinstitutt, Oslo, 1958).
17 Gow, A. J., *Int. Assoc. Sci. Hydrol.*, **61**, 272 (1963).

Isotopic Composition of Carbonates in a Marginal Marine Formation

THERE has been much interest in the use of the carbon and oxygen isotopic composition of fossils and limestones for determinations of palaeosalinities. We wish to show that, at least in marginal marine environments, fossils can have very different compositions from their matrix. Diagenesis has obliterated the record of depositional environment from the matrix, and whole rock samples should therefore not be used in palaeoecological isotope studies. Well preserved fossils, however, retain their isotopic composition.

Molluscs usually deposit their calcium carbonate shells in isotopic equilibrium with the dissolved bicarbonate of the water in which they live; and the oxygen is in equilibrium with the water itself[1,2]. Temperature also has an effect on the isotopic composition of the shell, but in most regions where freshwater–marine transitions have been studied this is outweighed by the large isotopic difference between marine and freshwater[3]. Thus fossil shells can be used to monitor changes in bicarbonate isotopic composition[4–6].

Many limestones are composed of the shells of invertebrates, and there is a clear distinction between the average carbon isotopic compositions of marine and freshwater limestones back into the Palaeozoic. The prevalence of freshwater diagenetic alteration of marine limestones, in the older rocks, has obliterated the oxygen isotope distinction that is shown by recent shells and geologically young limestones, and complex effects can also modify carbon isotope values; but Keith and Weber[7] were able to classify 80% of their large sample of palaeontologically determined marine or freshwater limestones correctly.

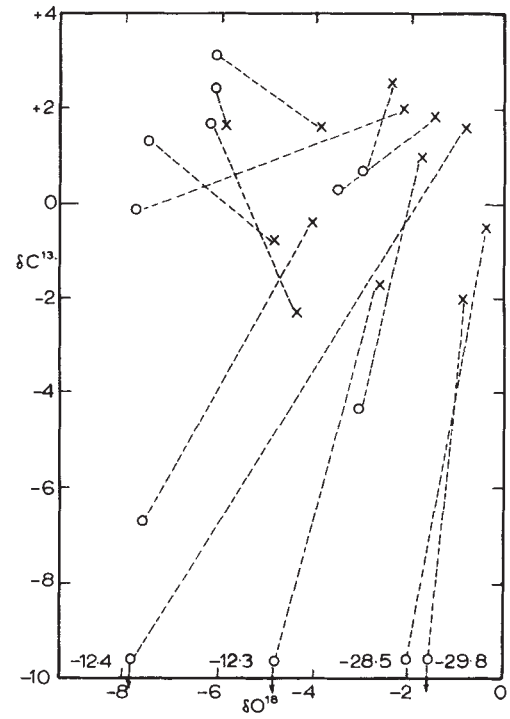

Fig. 1 Plot of $\delta^{13}C$ against $\delta^{18}O$ for fossil and matrix (for data see Table 1). *X*, fossil; *O*, matrix. Lines join fossils to their associated matrix values.

Although the rock will carry a record of diagenetic as well as depositional environment, many workers have shown that well preserved fossils retain their original isotopic composition in rocks as old as Mesozoic. This applies particularly to aragonitic mollusc shells, in which mineralogical preservation always seems to imply isotopic preservation[8], and also to coarsely crystalline calcitic skeletal elements such as belemnite rostra and oyster shells[9].

In an isotopic study of the Jurassic Great Estuarine Series of Scotland, Tan[10] has analysed both separated fossils and matrix samples from formations thought, on palaeontological grounds, to have accumulated in marginal-marine to freshwater environments[11,12]. In this context matrix refers simply to the rock that immediately surrounds the fossil; no distinction is made between the "primary" matrix (deposited with the fossil) and cement introduced later. Only the carbonate fraction of the matrix appears in the analysis. In most cases, large differences were observed between the fossil and its matrix, as shown in Table 1 and Fig. 1. Each pair of results is from a different bed in the succession.

We believe that the fossils are unaltered isotopically. Their compositions are reasonable in terms of expected palaeotemperatures and water isotopic compositions (F. C. Tan and J. D. Hudson, to be published), and the scatter of the values is much smaller than that of the matrices. The matrix can comprise various components, including fragments of fossils, fine grained calcite deposited along with the fossils but of different and commonly unknown origin, and sparry calcite cement. Only in the first case is it likely that its composition will approximate to that of the separated, unaltered fossils. In some rocks we can show petrographically that much of the matrix is sparry calcite cement of diagenetic origin and similar calcite that has replaced once-aragonitic shells (ref. 13 and F. C. Tan and J. D. Hudson, to be published).